Journal of
Manufacturing and Materials Processing

MDPI

Article

Processability and Physical Properties of Compatibilized Recycled HDPE/Rice Husk Biocomposites

Andrés Rigail-Cedeño [1,2,*], Miriam Lazo [1,2], Julio Gaona [1], Joshua Delgado [1], Clotario V. Tapia-Bastidas [1], Ana L. Rivas [1], Estephany Adrián [1,2] and Rodrigo Perugachi [1]

[1] Faculty of Mechanical Engineering and Production Science (FIMCP), ESPOL Polytechnic University, Guayaquil P.O. Box 09-01-5863, Ecuador; mdlazo@espol.edu.ec (M.L.); jgaona@espol.edu.ec (J.G.); aldebald@espol.edu.ec (J.D.); vtapia@espol.edu.ec (C.V.T.-B.); arivasfe@espol.edu.ec (A.L.R.); eadrian@espol.edu.ec (E.A.); cperugac@espol.edu.ec (R.P.)
[2] Plastics Processing Laboratory (PPL), ESPOL Polytechnic University, Guayaquil P.O. Box 09-01-5863, Ecuador
* Correspondence: arigail@espol.edu.ec

Abstract: The circular economy promotes plastic recycling, waste minimization, and sustainable materials. Hence, the use of agricultural waste and recycled plastics is an eco-friendly and economic outlook for developing eco-designed products. Moreover, new alternatives to reinforce recycled polyolefins and add value to agroindustrial byproducts are emerging to develop processable materials with reliable performance for industrial applications. In this study, post-consumer recycled high-density polyethylene (rHDPE) and ground rice husk (RH) of 20% *w*/*w* were blended in a torque rheometer with or without the following coupling agents: (i) maleic anhydride grafted polymer (MAEO) 5% *w*/*w*, (ii) neoalkoxy titanate (NAT) 1.5% *w*/*w*, and (iii) ethylene–glycidyl methacrylate copolymer (EGMA) 5% *w*/*w*. In terms of processability, the addition of RH decreased the specific energy consumption in the torque experiments with or without additives compared to neat rHDPE. Furthermore, the time to reach thermal stability in the extrusion process was improved with EGMA and MAEO compatibilizers. Tensile and impact test results showed that using coupling agents enhanced the properties of the RH composites. On the other hand, thermal properties analyzed through differential scanning calorimetry and thermogravimetric analysis showed no significant variation for all composites. The morphology of the tensile fracture surfaces was observed via scanning electron microscopy. The results show that these recycled composites are feasible for manufacturing products when an appropriate compatibilizer is used.

Keywords: recycled plastics; rice husk; agrowaste filler; compatibilizer

check for updates

Citation: Rigail-Cedeño, A.; Lazo, M.; Gaona, J.; Delgado, J.; Tapia-Bastidas, C.V.; Rivas, A.L.; Adrián, E.; Perugachi, R. Processability and Physical Properties of Compatibilized Recycled HDPE/Rice Husk Biocomposites. *J. Manuf. Mater. Process.* **2022**, *6*, 67. https://doi.org/10.3390/jmmp6040067

Academic Editor: Victor Neto

Received: 27 May 2022
Accepted: 17 June 2022
Published: 23 June 2022

Publisher's Note: MDPI stays neutral with regard to jurisdictional claims in published maps and institutional affiliations.

Copyright: © 2022 by the authors. Licensee MDPI, Basel, Switzerland. This article is an open access article distributed under the terms and conditions of the Creative Commons Attribution (CC BY) license (https://creativecommons.org/licenses/by/4.0/).

1. Introduction

Recycling is currently one of the most common strategies to reduce the adverse impact of polymeric material waste [1]. Moreover, this reduces harmful emissions into the environment, such as carbon dioxide and other chemical agents. It must be pointed out that every ton of recycled plastic saves approximately 3.8 barrels of oil [2] considering the carbon footprint of new polymers is greater than recycled material [3]. In addition, following circular global trends, recycling is gaining greater dynamism in the Ecuadorian plastic industry. Therefore, government regulations in Ecuador are pushing for the incorporation of recycled materials into the productive chain of the plastic industry.

Hidalgo-Crespo et al. [4] showed the average distribution of plastic waste in a domestic household with regard to plastic waste generation in Guayaquil (Ecuador). Figure 1 shows the proportion of primary plastics that have their final disposal in local landfills, with PET and HDPE/LDPE leading the list. However, mechanical recycling could tailor these materials by adding several dissimilar plastics incorporating additives or fillers to improve their processability properties or by developing new affordable materials to create innovative, more sustainable plastic products.

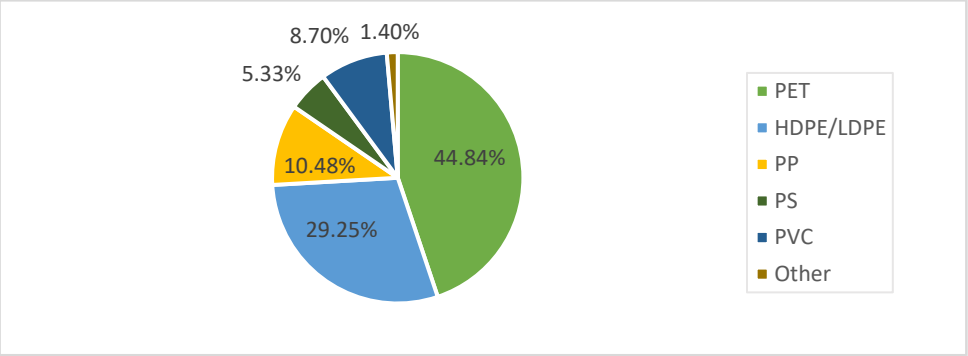


Figure 1. Distribution of primary plastic waste in Ecuador. Adapted from [4].

Globally, the plastic industry has incorporated organic and inorganic fillers for several years. Examples of organic fillers include wood or natural fibers, such as wheat straw, flax, sisal, or hemp [5,6]. For wood-based composites (WPC), polyethylene, polypropylene, and polyvinyl chloride have been widely used [7], but the WPC industry must deal with limited wood resources [8]. Consequently, designing naturally reinforced materials has become the main research scope for several types of green composites [9–11]. Although the development of these materials requires a thorough and separate evaluation of the properties of every component involved and the composite material, the use of natural fillers offers an eco-friendly alternative for synthetic materials.

In addition, agricultural waste has been used as a filler to solve pollution issues in several countries. These fillers are a more economical and suitable combination for polymer composites [12–14]. Rice husk (RH) has been gaining more use in plastics in recent years and is incorporated with thermoplastics and thermosets for industrial application [15]. Rice (*Oryza sativa*) is one of the principal agricultural products produced in Ecuador, with an average annual consumption of 50 kg per capita [16]. In 2019, rice plantations were distributed around the country, with the highlands and Amazon region accounting for 3.4% of production and coastal provinces accounting for 96.6%. By 2020, Guayas became the province with the highest rice yield, producing approximately 879,934 metric tons or 66% of the country's total production [17]. During paddy milling, rice husk represent 20% of the total weight of rice [18,19], meaning more than 200,000 tons of rice husk is generated in Ecuador every year. Several studies have shown that rice husk is mainly constituted of cellulose, hemicellulose, lignin, and silica, as detailed in Table 1. Due to its high silica content, degradation is slower than other agricultural byproducts [20]. Rice husk has little use other than animal feed, leaving a gap for potential applications in other industrial processes. Thus, the use of RH in the plastic industry is feasible in Ecuador.

Table 1. Basic rice husk composition.

References	Cellulose	Hemicellulose	Lignin	Moisture	Silica
Singh [21]	50	-	25–30	10–15	15–20
Chindaprasirt and Cao [22]	40	-	30	-	20
Gao et al. [23]	35–40	15–20	20–25	-	-
Martí-Ferrer et al. [24]	45	19	19.5	14	15

Polymer composites reinforced with natural fillers show poor mechanical properties when the adhesion of the fiber to the polymer is inadequate [25]. Research has shown that adding an appropriate compatibilizer to a polymer matrix can improve mechanical properties, including impact strength, ductility, tensile strength, and stiffness, because of improved interfacial bonding and compatibility [26,27]. Coupling agents based on functional groups such as maleic anhydride and glycidyl methacrylate have been extensively used to modify fiber or matrix and enhance the interfacial interaction [28]. Compatibilizers

incorporating maleic anhydride (or maleated polymers) overcome the incompatibility problem given the interactions between the anhydride groups of the compatibilizer and the hydroxyl groups of natural fillers, thus increasing tensile and flexural strengths of the composites [29]. For the case of RH polymer composites, a recent review performed by Suhot et al. [15] illustrated that most of the reported studies on the mechanical or moisture absorption kinetics of RH-reinforced composites were related to either RH modification or surface treatment before its incorporation into HDPE or other polymer matrices. However, few studies have correlated the feasibility of processing RH polymer composite using different coupling agents or recycled plastics toward manufacturing sustainable products.

This research assesses the effect of incorporating different commercial coupling agents in the manufacturing of recycled high-density polyethylene (rHDPE) and RH composites. The additives included those typically used in polymer compatibilization, such as bipolar copolymer (EGMA) and maleated copolymer (MAEO), and in in situ macromolecular catalysis (NAT). To determine the feasibility of processing/performance of the rHDPE/RH composites through extrusion processes, the specific energy consumption and shear viscosity were analyzed as well as the morphological, thermal, and mechanical properties of these composites.

2. Experimental

2.1. Materials

Ground rice husk (RH), which is used as reinforcement, was obtained from different artisanal rice mills in the Guayas province of Ecuador. Recycled high-density polyethylene (rHDPE) with melt flow index (MFI) of 3.96 g/10 min (190 °C/21.16 kg) was donated by Nutec Representaciones S.A. (Guayaquil, Ecuador). RETAIN™ 3000 (density of 0.87 g·cm^{-3}), a maleic anhydride grafted polymer (MAEO), was provided by ENTEC Latin America (Orlando, FL, USA). Ken-React® CAPS® L® 12/L neoalkoxy titanate (NAT) coupling agent (density of 0.95 g·cm^{-3}) was purchased from Kenrich Petrochemicals, Inc. (Bayonne, NJ, USA). LOTADER® AX8840 (MFI of 5 g/10 min at 190 °C/2.16 kg and a density of 0.94 g·cm^{-3}), an ethylene–glycidyl methacrylate copolymer (EGMA), was supplied by ARKEMA (Colombes, France). Additives and rHDPE were used as received.

2.2. Torque Rheometry

Before processing, all compounds were mixed manually in a beaker, as shown in Table 2. Additives were incorporated 5% *w*/*w*, except for the neoalkoxy titanate coupling agent, which was incorporated as suggested by the manufacturer.

Table 2. Recycled polyethylene/rice husk composite formulations (%).

Composite	rHDPE	RH	MAEO	NAT	EGMA
rHDPE	100	-	-	-	-
rHDPE/RH$_0$	80.0	20	-	-	-
rHDPE/RH$_1$	75.0	20	5	-	-
rHDPE/RH$_2$	78.5	20	-	1.5	-
rHDPE/RH$_3$	75.0	20	-	-	5

Composites were prepared in a Brabender Plastograph® EC torque rheometer with a process temperature of 185 °C at 60 rpm for 15 min. Rice husk was dried at 80 °C for 24 h before processing. Curves were obtained for every compound using BRABENDER® Mixer Program for Windows V4.9.8 and BRABENDER® Data Correlation V4.0.6 software (Duisburg, Germany).

Viscosity was determined through empirical equations considering the rheometer's geometry and processing variables. The constants relating to the geometry of the two-rotor mixer were obtained using Equation (1) [11]:

$$K_1 = \frac{1}{2\pi R_m^2 h} \; ; \; K_2 = \frac{2}{n R_m^{\frac{2}{n}} \left(R_i^{-\frac{2}{n}} - R_e^{-\frac{2}{n}} \right)} \tag{1}$$

where internal radius is R_i = 1.65 cm, external radius is R_e = 1.85 cm, mean radius is R_m = 1.75 cm), and height is h = 4.6 cm.

Thus, it can be observed that K_2 depends on n, which was determined in a torque vs. angular rotor speed (S) log–log plot. S was obtained through Equation (2) [30]:

$$S = \frac{2\pi R}{60} \tag{2}$$

where R is the average speed (rpm) of each test. Because this method is empirical, it is necessary to use the term "apparent" because it approximates the actual values of the rheological properties. The shear stress (τ) and shear rate ($\dot{\gamma}$), represented by Equations (3) and (4), respectively, were used [11]:

$$\tau = K_1 M \tag{3}$$

$$\dot{\gamma} = K_2 S \tag{4}$$

where M is the average torque from the software's torque vs. time graph provided for each test. Finally, the apparent viscosity (η) was determined according to Equation (5) [11]:

$$\eta = \frac{\tau}{\dot{\gamma}} \tag{5}$$

It is essential to highlight that these values belong to a constant speed of 60 rpm. Therefore, a representative equation of the power law must be developed for different speeds.

2.3. Test Specimen Preparation

Samples were cut manually, with the size determined in accordance with mechanical properties. Tensile (ASTM D638–type IV) and impact unnotched (ASTM D256) test specimens were molded using a hydraulic heat press for 10 min at 180 °C and 8.3 MPa. After the specified time, keeping the pressure constant, specimens were cooled down to 155 °C at a constant rate of 5 °C·min^{-1}. When the equipment reached the set temperature, samples were immersed in water at room temperature for three minutes before unmolding. Figure 2 shows the test specimens and pellets obtained.

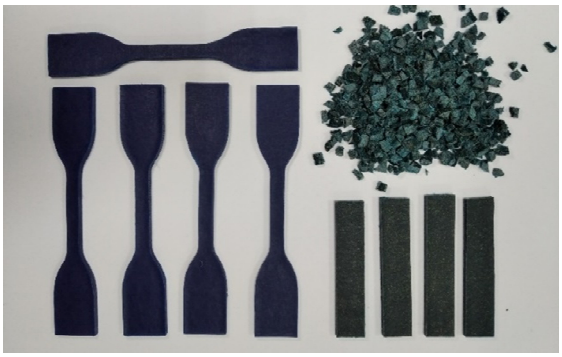


Figure 2. Composite samples: rHDPE tensile test specimens (**left**), rHDPE/RH_0 impact unnotched test specimens (**right bottom corner**), and rHDPE/RH_1 pellets (**right upper corner**).

2.4. Characterization and Evaluation

2.4.1. Rice Husk Granulometry

Rice husk underwent morphological analysis for particle size distribution. A RETSCH laboratory sieve shaker (Haan, Germany) was operated at 50 Hz using different sieve opening sizes (850, 500, 300, 212, 150, 106, and 75 µm) for 10 min.

2.4.2. Scanning Electron Microscopy (SEM)

Fractured tensile test specimens and rice husk morphology were observed through an FEI Inspect S50 scanning electron microscope (Hillsboro, OR, USA) in high vacuum mode using the backscattering detector at a voltage of 10.5 kV (4.5 spot). Micrographs were obtained through xT Microscope Server Version 3.1.4 software.

2.4.3. Differential Scanning Calorimetry (DSC)

Transition temperatures and enthalpies were analyzed in a TA Instruments Q200 DSC analyzer (New Castle, USA). Double run experiments were performed from 23 to 200 °C at a constant rate of 10 °C·min^{-1} (nitrogen flow of 50 mL·min^{-1}). The degree of crystallinity (Xc) was measured using the enthalpy of fusion (H_f) and rHDPE weight fraction (ω) in the composite, as shown in Equation (6) [31]. Theoretical melting enthalpy (H_f^o) for completely crystalline HDPE is 293 J·g^{-1}.

$$X_c = \frac{H_f}{H_f^o \times \omega} \times 100 \quad (6)$$

2.4.4. Thermogravimetric Analysis (TGA)

The thermal stability of the composites and rice husk was measured using a TA Instruments Q600 STD (TGA/DSC) analyzer. Samples of approximately 15 mg were tested under ultra-high-purity nitrogen atmosphere (100 mL·min^{-1}). The experiment was run from room temperature to 600 °C with a heating ramp of 20 °C·min^{-1}.

2.4.5. Mechanical Properties

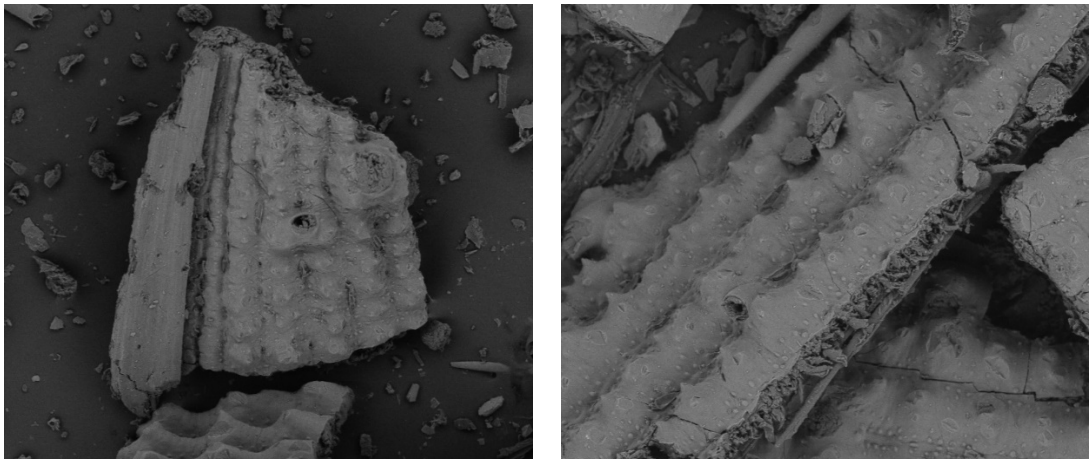
Tensile properties were assessed following ASTM D638 in Shimadzu AG-IS (10 kN) universal test frame. Data were collected and processed through TRAPEZIUM2 V2.24 software applying a test speed of 50 mm·min^{-1}. Impact resistance tests were performed on unnotched specimens according to ASTM D256. Jin Jian standard pendulum was operated at a speed of 3.50 m·s^{-1}.

3. Results and Discussion

3.1. Rice Husk Characterization

Micrographs showing rice husk's surface morphology at 400× and 500× magnification are displayed in Figure 3. Over the outer face of the particle, bump-like structures were arranged in an orderly pattern. According to Chen et al. [32], this area is mainly constituted of silica. On the other hand, the inner section of the RH (Figure 3b), which exhibited irregular alignment, is composed mostly of cellulose and lignin [33].

Figure 4 presents the particle distribution for the rice husk passed through sieves. In general, 96.2% of the sample had a particle size smaller than 850 µm. More than 50% of the rice husk passed through the sieves had a particle size between 300 and 850 µm, with 31% of these being between 300 and 500 µm.



(**a**) (**b**)

Figure 3. Rice husk micrographs: (**a**) 400× and (**b**) 500× magnification.

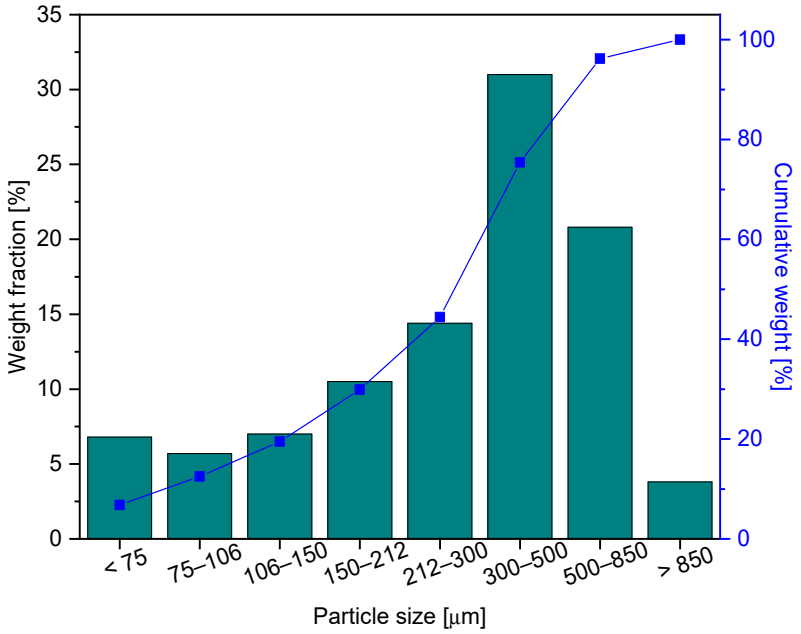


Figure 4. Rice husk particle distribution.

The thermal profile for rice husk is shown in Figure 5. As can be seen, there are four stages in the TG curve: volatile loss and three degradation stages. Between 23 and 150 °C, the weight loss can be attributed to absorbed water and other volatiles [34]. Because the sample was dried beforehand, the mass loss for this phase was less than 3.5%. A first, slight degradation stage occurred at 150–250 °C. Because the weight loss rate of 0.15%/°C is low, the initial degradation can be attributed to that of lignocellulosic components [35]. At the second stage of degradation, from 250 to 400 °C, the sample underwent an active pyrolysis step where 48% of its mass was lost. The weight loss rate (DTG) curve showed the highest peak at 341.33 °C and a shoulder peak at 303.12 °C, indicating the maximum degradation of cellulose and hemicellulose, respectively [36]. At the final stage, at 400 °C, lignin decomposition continued at a lower rate of 0.04%/°C. Unlike cellulose and hemicellulose, lignin's pyrolysis occurs at a broader temperature range (about 100–900 °C) and at an average rate of 0.14%/°C [37]. The 44.42% residue should include silica, char, and lignin byproducts.

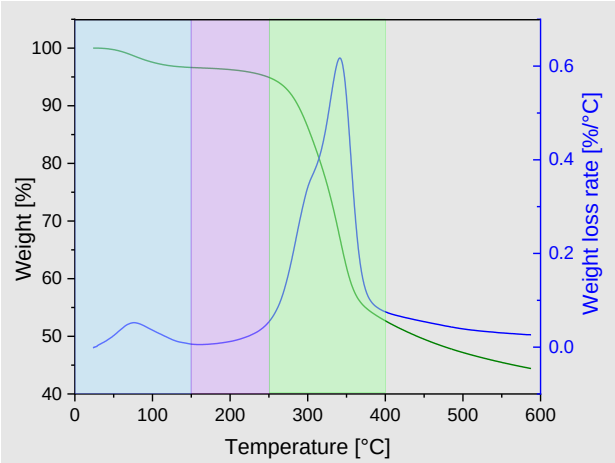


Figure 5. TG/DTG for rice husk.

3.2. Torque Rheometry and Processability Analysis

Figure 6a shows the stock temperature behavior due to the presence of the rice husk during extrusion processing. The observed temperature change related to the melting temperature inside the mixer chamber may be attributed to a modification in the composite's properties during processing. The presence of rice husk, which is rich in silica, decreased the stock temperature after 3 min of processing compared to neat rHDPE. RH has been observed to increase the thermal stability of the polymer matrices [15] due to its insulating properties. It has been observed that inorganic materials can decrease the melting temperature of polyolefin single extrusion process [38], so RH was able to reduce the stock temperature in these rHDPE polymer composites.

Processability, defined by Sisanth et al. [39] as "the behavior and interactions of polymer, filler, and other additives during various processing stages", depends on cure characteristics and rheological properties. In this case, the processability was related to the ability to process biocomposites by conventional melting process technologies such as extrusion, compression, or injection molding to study the typical parameters used in the plastic processing industry. The main parameters analyzed to evaluate processability were torque, specific energy, viscosity, and time needed for stability at an extrusion rate of 60 rpm and processing time of 15 min, as seen in Table 3. From the torque curve in Figure 6b, the highest loading torque value of 60.4 N·m was obtained when rice husk was added to the rHDPE matrix. With the addition of this filler, the initial mobility of the polyethylene chains appeared to be limited, increasing the initial fusion torque [40]. Even so, the reinforced composites presented lower shear viscosity when they reached a molten state at about 23 N·m by the end of the test. In contrast, neat rHDPE stabilized at 28 N·m. A decrease in viscosity of the reinforced composites can be ascribed to a lubricating effect of the migration of RH components with low molecular weight or wall slip changes due to the dispersion of RH particles [41].

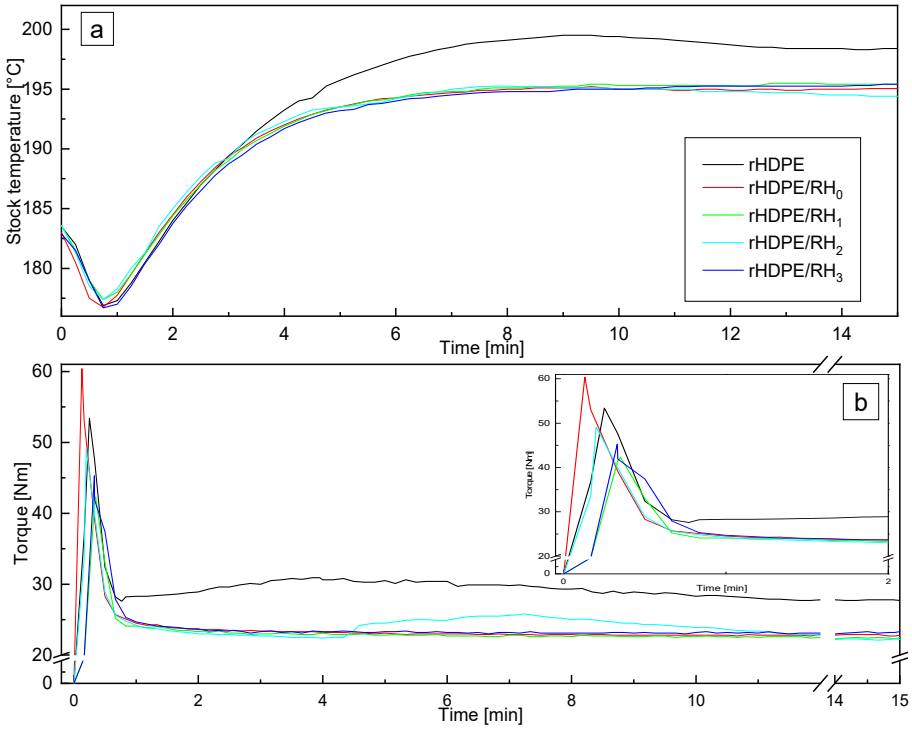


Figure 6. Fusion curves: (**a**) stock temperature vs. time and (**b**) torque vs. time for neat rHDPE and reinforced composites.

Table 3. Fusion behavior for neat and filled rHDPE.

Composite	Loading/Max Torque (N·m)	Specific Energy (kN·m/kg)	Viscosity at 60 rpm (Pa·s)	Time Needed Stability (Min)	Processing Time (Min)
rHDPE	53.4 ± 0.7	4656.8 ± 13.6	6473.8	13.5	15
rHDPE/RH_0	60.4 ± 1.0	3790.8 ± 4.6	6113.5	12.5	15
rHDPE/RH_1	42.3 ± 0.4	3642.4 ± 23.3	5330.7	12.0	15
rHDPE/RH_2	49.1 ± 0.6	3837.1 ± 21.2	5055.0	-	15
rHDPE/RH_3	45.3± 0.1	3755.7 ± 12.9	5675.0	11.5	15

The steady state establishes a stable condition for the material's morphology [42]. Reducing the time to reach this state is essential to optimize processing time and prevent degradation. Stabilization time for most experiments was reached between 11.5 and 13.5 min, with the materials displaying similar rheological behavior. However, the rHDPE/RH_2 composite did not stabilize even after 15 min of processing. Furthermore, it presented an increase in torque of 25.8 N·m between 4.5 and 11.5 min. This phenomenon observed on rHDPE/RH_2 can generally be attributed to increased interaction between the additive, polymer, and fiber. The torque increased in the NAT biocomposite, but this behavior was not reflected in the process temperature. Research on different coupling agents addresses this torque increase as catalysis [43] or reactive compatibilization [44], where the additive reacts with the polymer and bonds with the filler.

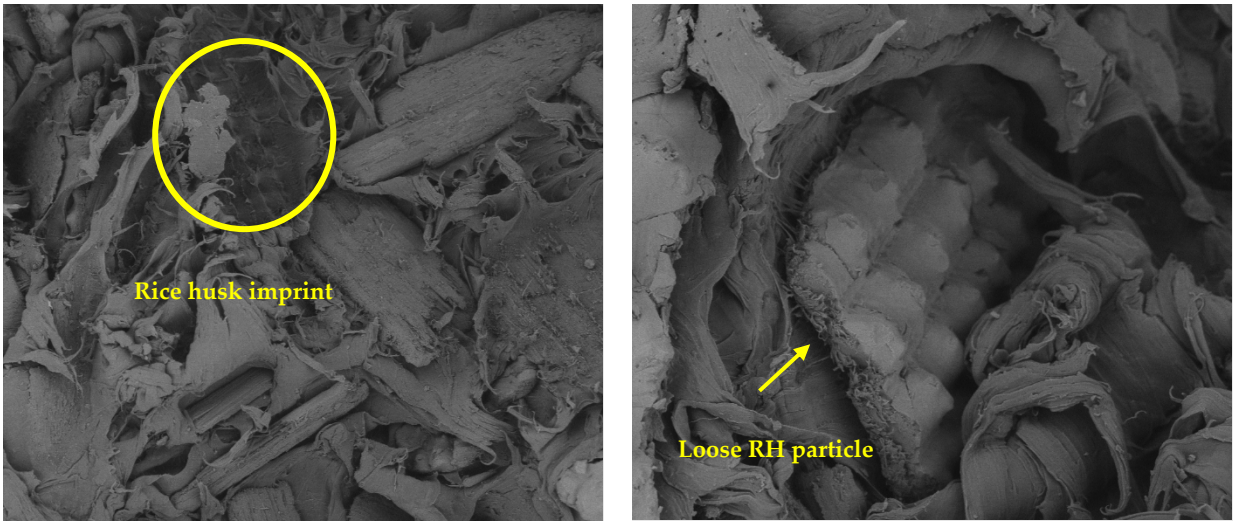
In general, when polymer is melted, the presence of RH increases the melt density of the composite, so shear force increases. However, viscous dissipation was affected by the insulating capacity of the RH, reducing viscosity, torque, and stock temperature. In addition, the effect of the coupling agent decreased the resistance to flow, so the viscosity, specific energy, and torque were diminished, except for the NAT biocomposite.

The rHDPE/RH_1 and rHDPE/RH_3 composites exhibited the lowest stabilization time and specific energy values. Moreover, given that rHDPE/RH_0 high fusion peak is not

beneficial to processability, EGMA and MAEO coupling agents could act as a process aid to optimize the operation of transformation processes that require lower viscosity [45].

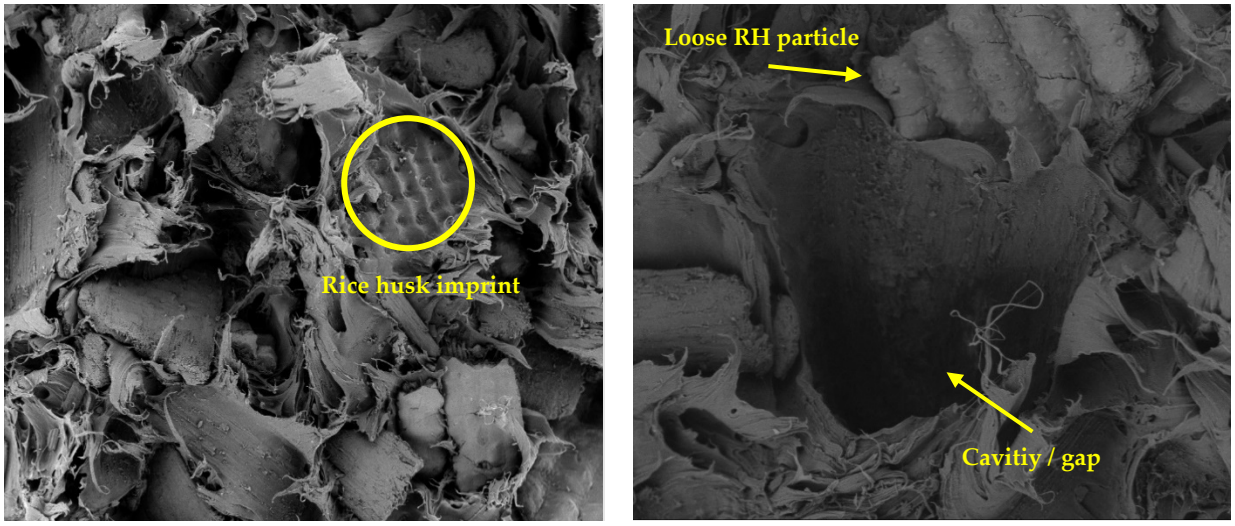
3.3. Scanning Electron Microscopy

The morphology of the reinforced composites after tensile evaluation is displayed in Figures 7–10. In Figure 7a, an imprint of the RH outer surface can be found. The RH surface mark is also noticeable for rHDPE/RH_1 and rHDPE/RH_2 in Figure 8a or Figure 9a, respectively. However, RH residue and irregularities can be seen due to the pull-out phenomenon on MAEO and NAT composites. The enhancement of this phenomenon is due to the improved compatibility produced between the rice husk and the polyethylene [24].



(**a**) (**b**)

Figure 7. SEM micrographs for reinforced composite rHDPE/RH_0 (**a**) 200× and (**b**) 500× magnification.



(**a**) (**b**)

Figure 8. SEM micrographs for reinforced composite rHDPE/RH_1 (**a**) 200× and (**b**) 400× magnification.

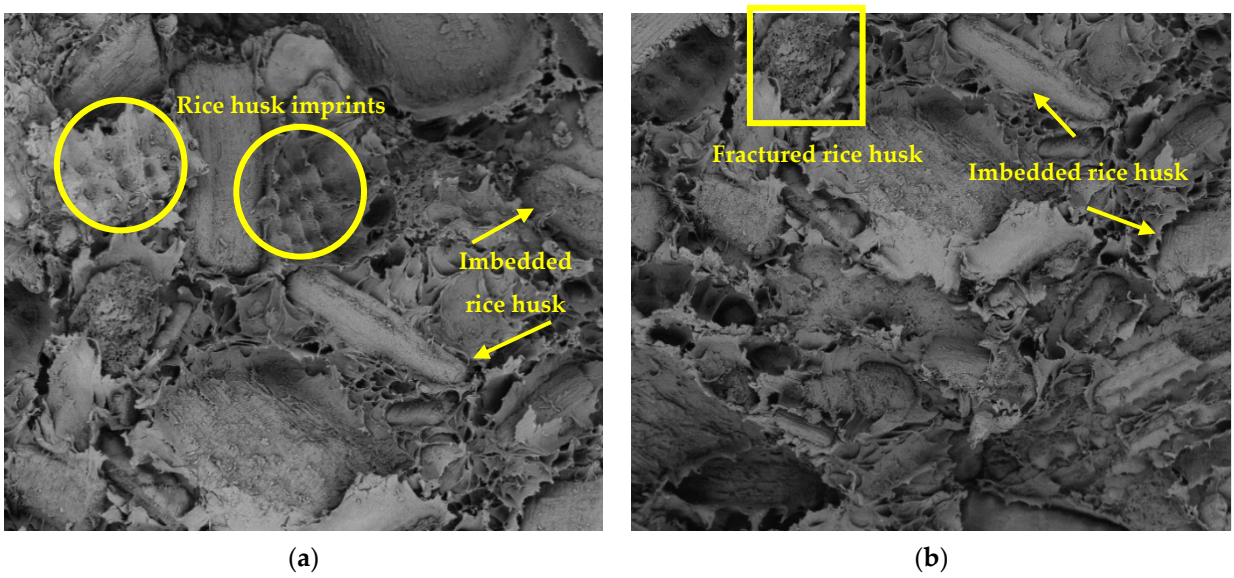


Figure 9. SEM micrographs for reinforced composite rHDPE/RH_2 (**a**) 200× and (**b**) 180× magnification.

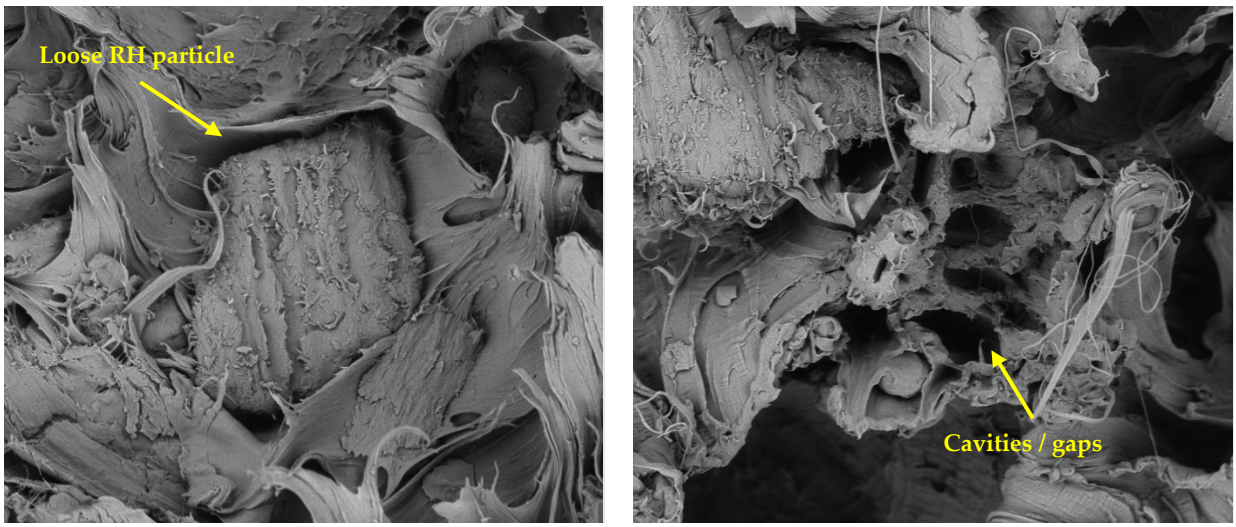


Figure 10. SEM micrographs for reinforced composite rHDPE/RH_3 1000× magnification.

As can be observed in Figure 7b, the rice husk was loosely attached to the polymer matrix. The composites incorporating EGMA and MAEO showed stronger compatibility than rHDPE/RH_0, as illustrated in Figures 8 and 10, respectively. Nevertheless, both composites displayed gaps in their microstructures. Fiber pull-out could be more frequent during fracture because of the poor interaction between polymer and filler [46].

Figure 9b shows fractured rice husk particles, indicating good interfacial interaction between fiber and polyolefin [47]. In addition, the RH was distinctly embedded in the rHDPE matrix compared to the other composites. As can be seen in Figures 7, 8, and 10, a ductile deformation occurred until breakage, whereas rHDPE/RH_2 appeared to have a brittle fracture during the tensile test. This unusual behavior for this matrix might have resulted from the catalysis provoked by the NAT coupling agent [43].

3.4. Thermal Properties

Transition temperatures, enthalpy changes, and degree of crystallinity (X_c) of the samples are shown in Table 4. Reductions in melting temperatures (T_m) when using rice fibers as polyolefin fillers have been described in the literature [48]. The rHDPE/RH_3 presented a slight reduction in melting temperature. This reduction could be attributed to

enhanced compatibility of EGMA as well as to the additive's lower molecular weight [49]. The latter implies diminished thermal properties as the heat necessary for melting would be lower.

Table 4. Thermal properties of rHDPE and reinforced composites.

Composite	T_m (°C)	T_c (°C)	H_f (J·g^{-1})	H_c (J·g^{-1})	X_c (%)
rHDPE	134.23 ± 0.99	115.14 ± 0.97	157.90 ± 5.10	198.70 ± 1.30	53.89 ± 0.87
rHDPE/RH$_0$	134.74 ± 0.69	114.70 ± 0.91	125.85 ± 1.75	161.25 ± 2.65	53.69 ± 0.75
rHDPE/RH$_1$	135.33 ± 0.60	115.84 ± 0.53	124.95 ± 0.55	151.40 ± 0.60	56.86 ± 0.25
rHDPE/RH$_2$	134.10 ± 0.38	114.55 ± 0.26	129.40 ± 0.80	157.50 ± 0.79	56.26 ± 0.35
rHDPE/RH$_3$	133.14 ± 0.87	116.41 ± 0.09	122.50 ± 4.57	157.25 ± 0.35	53.90 ± 1.66

Enthalpy of fusion (H_f) and crystallization (H_c) of the rHDPE decreased for the reinforced composites. However, this change was mainly due to the percentage of polyethylene in the samples [50].

Research has demonstrated that organic fillers affect polymer crystallinity [51] because molecules are less free to move during crystallization [48]. However, incorporating rice husk into the HDPE matrix showed no significant change regarding crystallinity. In contrast, MAEO and NAT coupling agents increased X_c. The use of maleic anhydride copolymers has been proved to increase crystallinity due to its ability to promote the interaction between the organic filler and polymer [52]. On the other hand, the neoalkoxy titanate coupling agent increases crystallinity when filler concentrations are relatively low [53]. In general, enhanced compatibility will result in an increase in enthalpy and a higher degree of crystallinity.

Figure 11 displays the TG and DTG curves of each composite. Recycled HDPE experienced a single-step degradation process with dramatic weight loss between 420 and 510 °C at approximately 3%/°C. After 600 °C, the residue left was about 0.5%. Given that rHDPE molecules break down into gaseous byproducts [8], the sample reported the least residue.

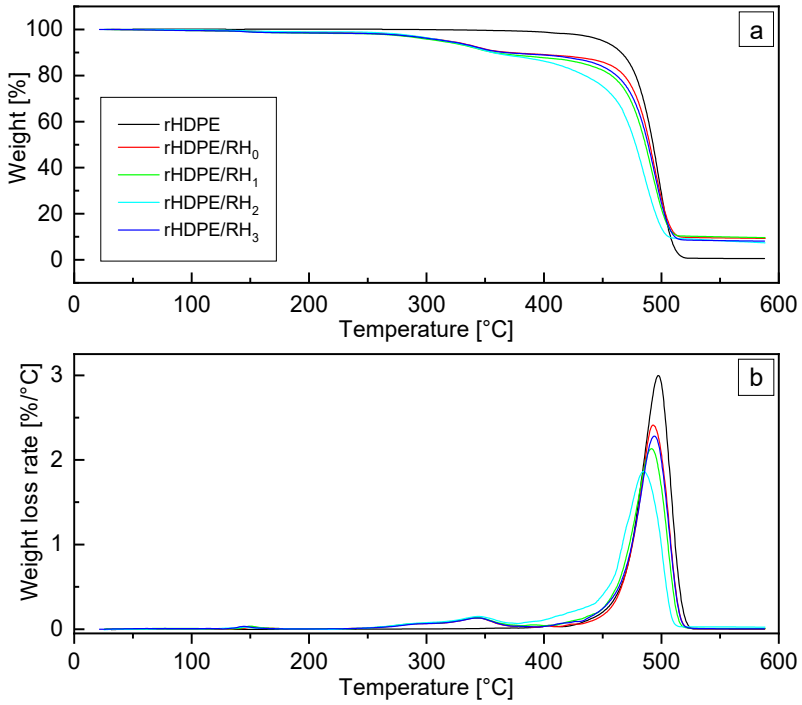


Figure 11. (**a**) TG, (**b**) DTG for rHDPE/RH composites.

On the other hand, reinforced composites exhibited a two-step thermal degradation. From 250 to 400 °C, the weight loss can be mainly attributed to rice husk (Figure 5). The second stage was defined by the rHDPE matrix. Reported variations in mass loss and maximum rate of weight loss (DTG_{max}) were due to the thermal stability of the coupling agents. The NAT composite showed an early beginning for the polymer degradation phase. Among the compatibilized composites, rHDPE/RH_3 presented the higher DTG_{max} of 494.39 °C, followed closely by rHDPE/RH_1 with 491.50 °C. Despite the influence of additives on the rHDPE/RH thermal behavior, HDPE process temperatures were lower than the ones observed in the thermograms.

3.5. Mechanical Properties

Tensile and impact values for rHDPE and reinforced composites are presented in Table 5. Neat rHDPE exhibited a ductile behavior with an elasticity modulus of 0.929 GPa and ultimate strength of 23.78 MPa. These properties were significantly affected by adding 20% of rice husk. The tensile strength decreased to 20.48 MPa, while Young's modulus increased by 18.77%. The polarity difference between the filler and the polymer matrix reduced the tensile strength due to poor filler–matrix adhesion, interfering the stress transfer [52]. The use of compatibilizers slightly increased the tensile modulus of the reinforced composites. Although incorporating 5% of MAEO decreased the ultimate strength to 17.66 MPa, NAT and EGMA coupling agents increased the maximum strength, obtaining 26.77 and 24.15 MPa, respectively. Effective polymer additive/fiber interaction improves tensile stress [54] as adhesion is enhanced. The elasticity modulus increased for all reinforced composites. Due to the high stiffness of the organic filler, polymer matrix mobility was restricted. In this matter, interfacial interaction has little influence on tensile modulus when compared to ultimate strength [55].

Table 5. Tensile and impact properties of rHDPE and reinforced composites.

Composite	Ultimate Strength (MPa)	Young's Modulus (GPa)	Impact Strength ($J \cdot m^{-1}$)
rHDPE	23.8 ± 0.1	0.93 ± 0.1	173.3 ± 7.9
rHDPE/RH_0	20.5 ± 0.4	1.10 ± 0.0	45.38 ± 2.1
rHDPE/RH_1	17.7 ± 0.4	1.02 ± 0.1	70.94 ± 3.6
rHDPE/RH_2	27.5 ± 0.5	0.99 ± 0.1	59.23 ± 2.2
rHDPE/RH_3	24.5 ± 0.3	1.04 ± 0.1	87.18 ± 5.0

Neat rHDPE presented an impact strength of 173.3 $J \cdot m^{-1}$, which decreased to 45.38 $J \cdot m^{-1}$ when rice husk was incorporated into the polyethylene matrix. A low interfacial adhesion between the filler and polymer could provoke microcracks at the impact point, promoting crack propagation during the test [56]. These microcracks result in impact energy reduction. Similarly, RH particles become a source of stress concentrators and affect the energy absorption efficiency [57].

Coupling agents enhanced the impact strength of reinforced rHDPE. EGMA and MAEO increased this property to 92 and 56%, respectively. Previous studies [25,58] have shown that better wetting and compatibilization of the filler to the polymer matrix prevent the propagation of cracks. Titanate coupling agent also improves impact energy absorption but only by 30%. Rodríguez et al. [59] also showed better enhancement of impact strength on polyolefin reinforced with organic fibers when using maleic anhydride rather than a titanate-based coupling agent.

4. Conclusions

Rice husk was incorporated into the rHDPE matrix via a stationary torque rheometer. The addition of RH filler reduced viscosity and torque at extrusion shear rates, increasing the feasibility of applying extrusion process for this family of biocomposites. The specific energy was reduced in the presence of RH and coupling agents from 4656.8 kN·m/kg for

neat rHDPE to an average of 3800 kN·m/kg for reinforced composites. Thus, production costs should be decreased due to low-cost RH/rHDPE and reduced cost of energy processing. EGMA and MAEO coupling agents decreased the fusion torque of reinforced composites from 60.4 to 42.3 and 45.3 N·m, respectively, showing it is suitable for transformation processes requiring lower shear viscosity. Micrographs showed poor adhesion between the fiber–polymer systems. Polar coupling agents demonstrated enhancement of interfacial interaction. Thermal stability was affected by incorporation of organic filler, presenting an early, additional degradation stage between 250 and 400 °C. Improvement in impact properties of the RH composite was observed with MAEO, NAT, and EGMA coupling agents (up to 92%). According to the results, rice husk is feasible for developing extruded bio-based composites and process energy optimization when coupling agents are incorporated. Additionally, rice husk could serve as an eco-friendlier alternative to wood in WPC, especially in regions where rice is one of the main food supplies for the population. Furthermore, WPC and RH biocomposites showed similar mechanical properties, namely good tensile resistance with lower elasticity and impact strength. This study provides the groundwork for future research on the effect of RH particle size, filler concentration, and novel coupling agents on the processability of rHDPE/RH-reinforced composites and puts forward interesting areas to be investigated for other reinforced polyolefins.

Author Contributions: Conceptualization, A.R.-C., C.V.T.-B. and A.L.R.; data curation, M.L. and J.G.; formal analysis, M.L., J.G. and J.D.; funding acquisition, A.R.-C., E.A. and R.P.; investigation, A.R.-C., M.L., J.G. and J.D.; methodology, A.R.-C., M.L., J.G. and J.D.; project administration, A.R.-C.; resources, A.R.-C. and E.A.; supervision, A.R.-C.; visualization, A.R.-C. and M.L.; writing—original draft, A.R.-C., M.L. and J.G.; writing—review and editing, A.R.-C., M.L. and C.V.T.-B. All authors have read and agreed to the published version of the manuscript.

Funding: This research received no external funding.

Institutional Review Board Statement: Not applicable.

Informed Consent Statement: Not applicable.

Data Availability Statement: Not applicable.

Acknowledgments: The authors express their gratitude and appreciation to the Laboratory of Testing Materials (LEMAT) and the Center of Nanotechnology Research and Development (CIDNA) for supporting our research during material evaluation and characterization.

Conflicts of Interest: The authors declare no conflict of interest.

References

1. Hopewell, J.; Dvorak, R.; Kosior, E. Plastics recycling: Challenges and opportunities. *Philos. Trans. R. Soc. B Biol. Sci.* **2009**, *364*, 2115–2126. [CrossRef] [PubMed]
2. Marish Kumar, P.; Indu Sailaja, K.A.; Lydia, J.; Suganya, D. Automated plastic bottle recycling machine. *Test Eng. Manag.* **2020**, *82*, 5402–5408.
3. Zheng, J.; Suh, S. Strategies to reduce the global carbon footprint of plastics. *Nat. Clim. Chang.* **2019**, *9*, 374–378. [CrossRef]
4. Hidalgo-Crespo, J.; Amaya, J.L.; Soto, M.; Caamaño-Gordillo, L. Domestic Plastic Waste in the City of Guayaquil: Generation Rate and Classification. In Proceedings of the 19th LACCEI International Multi-Conference for Engineering, Education, and Technology, Buenos Aires, Argentina, 21–23 July 2021.
5. Yu, M.; Mao, H.; Huang, R.; Ge, Z.; Tian, P.; Sun, L.; Wu, Q.; Sun, K. Mechanical and thermal properties of r-high density polyethylene composites reinforced with wheat straw particleboard dust and basalt fiber. *Int. J. Polym. Sci.* **2018**, *2018*, 5101937. [CrossRef]
6. Gholampour, A.; Ozbakkaloglu, T. A review of natural fiber composites: Properties, modification and processing techniques, characterization, applications. *J. Mater. Sci.* **2020**, *55*, 829–892. [CrossRef]
7. Youssef, A.M.; El-Gendy, A.; Kamel, S. Evaluation of corn husk fibers reinforced recycled low density polyethylene composites. *Mater. Chem. Phys.* **2015**, *152*, 26–33. [CrossRef]
8. Chen, R.S.; Ahmad, S. Mechanical performance and flame retardancy of rice husk/organoclay-reinforced blend of recycled plastics. *Mater. Chem. Phys.* **2017**, *198*, 57–65. [CrossRef]
9. Chun, K.S.; Husseinsyah, S. Agrowaste-based composites from cocoa pod husk and polypropylene. *J. Thermoplast. Compos. Mater.* **2016**, *29*, 1332–1351. [CrossRef]

10. Obasi, H.C. Peanut husk filled polyethylene composites: Effects of filler content and compatibilizer on properties. *J. Polym.* **2015**, *2015*, 189289. [CrossRef]
11. Koay, S.C.; Chan, M.Y.; Pang, M.M.; Tshai, K.Y. Influence of filler loading and palm oil-based green coupling agent on torque rheological properties of polypropylene/cocoa pod husk composites. *Adv. Polym. Technol.* **2018**, *37*, 2246–2252. [CrossRef]
12. Maraveas, C. Production of sustainable and biodegradable polymers from agricultural waste. *Polymers* **2020**, *12*, 1127. [CrossRef] [PubMed]
13. Acquavia, M.; Pascale, R.; Martelli, G.; Bondoni, M.; Bianco, G. Natural polymeric materials: A solution to plastic pollution from the agro-food sector. *Polymers* **2021**, *13*, 158. [CrossRef] [PubMed]
14. Salazar-Cruz, B.A.; Chávez-Cinco, M.Y.; Morales-Cepeda, A.B.; Ramos-Galván, C.E.; Rivera-Armenta, J.L. Evaluation of thermal properties of composites prepared from pistachio shell particles treated chemically and polypropylene. *Molecules* **2022**, *27*, 426. [CrossRef] [PubMed]
15. Suhot, M.A.; Hassan, M.Z.; Aziz, S.A.; Md Daud, M.Y. Recent progress of rice husk reinforced polymer composites: A review. *Polymers* **2021**, *13*, 2391. [CrossRef]
16. Agricultural Public Information System (SIPA). *Food Balance Sheet*; SIPA: Quito, Ecuador, 2021.
17. Agricultural Public Information System (SIPA). *Surface and Production—INEC*; SIPA: Quito, Ecuador, 2021.
18. Chand, N.; Fahim, M. Natural Fibers and Their Composites. In *Tribology of Natural Fiber Polymer Composites*; Elsevier: Amsterdam, The Netherlands, 2021; pp. 1–59.
19. López-Alonso, M.; Martín-Morales, M.; Martínez-Echevarría, M.J.; Agrela, F.; Zamorano, M. Residual Biomasses as Aggregates Applied in Cement-Based Materials. In *Waste and Byproducts in Cement-Based Materials*; Elsevier: Amsterdam, The Netherlands, 2021; pp. 89–137.
20. Kumar, M.; Mishra, P.K.; Upadhyay, S.N. Thermal degradation of rice husk: Effect of pre-treatment on kinetic and thermodynamic parameters. *Fuel* **2020**, *268*, 117164. [CrossRef]
21. Singh, B. Rice Husk Ash. In *Waste and Supplementary Cementitious Materials in Concrete*; Elsevier: Amsterdam, The Netherlands, 2018; pp. 417–460.
22. Chindaprasirt, P.; Cao, T. The Properties and Durability of High-Pozzolanic Industrial by-Products Content Concrete Masonry Blocks. In *Eco-Efficient Masonry Bricks and Blocks*; Elsevier: Amsterdam, The Netherlands, 2015; pp. 191–214.
23. Gao, Y.; Guo, X.; Liu, Y.; Fang, Z.; Zhang, M.; Zhang, R.; You, L.; Li, T.; Liu, R.H. A full utilization of rice husk to evaluate phytochemical bioactivities and prepare cellulose nanocrystals. *Sci. Rep.* **2018**, *8*, 10482. [CrossRef]
24. Martí-Ferrer, F.; Vilaplana, F.; Ribes-Greus, A.; Benedito-Borrás, A.; Sanz-Box, C. Flour rice husk as filler in block copolymer polypropylene: Effect of different coupling agents. *J. Appl. Polym. Sci.* **2006**, *99*, 1823–1831. [CrossRef]
25. Fávaro, S.L.; Lopes, M.S.; Vieira de Carvalho Neto, A.G.; Rogério de Santana, R.; Radovanovic, E. Chemical, morphological, and mechanical analysis of rice husk/post-consumer polyethylene composites. *Compos. Part A Appl. Sci. Manuf.* **2010**, *41*, 154–160. [CrossRef]
26. Chen, R.S.; Ahmad, S.; Gan, S. Characterization of rice husk-incorporated recycled thermoplastic blend composites. *BioResources* **2016**, *11*, 8470–8482. [CrossRef]
27. Ghosh, A. Performance modifying techniques for recycled thermoplastics. *Resour. Conserv. Recycl.* **2021**, *175*, 105887. [CrossRef]
28. Panthapulakkal, S.; Sain, M.; Law, S. Effect of coupling agents on rice-husk-filled HDPE extruded profiles. *Polym. Int.* **2005**, *54*, 137–142. [CrossRef]
29. De Carvalho, F.P.; Isabel Felisberti, M.; Soto Oviedo, M.A.; Davila Vargas, M.; Farah, M.; Fortes Ferreira, M.P. Rice husk/poly(propylene-co-ethylene) composites: Effect of different coupling agents on mechanical, thermal, and morphological properties. *J. Appl. Polym. Sci.* **2012**, *123*, 3337–3344. [CrossRef]
30. Ari, G.A.; Aydin, I. Rheological and fusion behaviors of PVC micro- and nano-composites evaluated from torque rheometer data. *J. Vinyl Addit. Technol.* **2010**, *16*, 223–228. [CrossRef]
31. Orji, B.O.; McDonald, A.G. Evaluation of the mechanical, thermal and rheological properties of recycled polyolefins rice-hull composites. *Materials* **2020**, *13*, 667. [CrossRef]
32. Chen, Z.; Xu, Y.; Shivkumar, S. Microstructure and tensile properties of various varieties of rice husk. *J. Sci. Food Agric.* **2018**, *98*, 1061–1070. [CrossRef] [PubMed]
33. Bie, R.S.; Song, X.F.; Liu, Q.Q.; Ji, X.Y.; Chen, P. Studies on effects of burning conditions and rice husk ash (rha) blending amount on the mechanical behavior of cement. *Cem. Concr. Compos.* **2015**, *55*, 162–168. [CrossRef]
34. Li, X.-Y.; Guo, T.-S.; Li, M.-F.; Peng, F. Comparison of structure, thermal stability, and pyrolysis products of lignin extracted with chcl-formic acid/lactic acid systems. *J. Mater. Res. Technol.* **2021**, *14*, 841–850. [CrossRef]
35. El-Sayed, S. Thermal decomposition, kinetics and combustion parameters determination for two different sizes of rice husk using TGA. *Eng. Agric. Environ. Food* **2019**, *12*, 460–469. [CrossRef]
36. Amit, T.A.; Roy, R.; Raynie, D.E. Thermal and structural characterization of two commercially available technical lignins for potential depolymerization via hydrothermal liquefaction. *Curr. Res. Green Sustain. Chem.* **2021**, *4*, 100106. [CrossRef]
37. Yang, H.; Yan, R.; Chen, H.; Lee, D.H.; Zheng, C. Characteristics of hemicellulose, cellulose and lignin pyrolysis. *Fuel* **2007**, *86*, 1781–1788. [CrossRef]
38. Rigail-Cedeño, A.; Vera-Sorroche, J.; García-Mejía, G.; Intriago, R. Effect of the intercalation and dispersion of organoclays on energy demand in the extrusion of recycled HDPE/PP nanocomposites. *Energies* **2022**, *15*, 859. [CrossRef]

39. Sisanth, K.S.; Thomas, M.G.; Abraham, J.; Thomas, S. General Introduction to Rubber Compounding. In *Progress in Rubber Nanocomposites*; Elsevier: Amsterdam, The Netherlands, 2017; pp. 1–39.
40. Manaia, J.P.; Manaia, A. Interface modification, water absorption behaviour and mechanical properties of injection moulded short hemp fiber-reinforced thermoplastic composites. *Polymers* **2021**, *13*, 1638. [CrossRef] [PubMed]
41. Barczewski, M.; Lewandowski, K.; Rybarczyk, D.; Kloziński, A. Rheological and single screw extrusion processability studies of isotactic polypropylene composites filled with basalt powder. *Polym. Test.* **2020**, *91*, 106768. [CrossRef]
42. Freire, E.; Bianchi, O.; Monteiro, E.E.C.; Reis Nunes, R.C.; Forte, M.C. Processability of PVDF/PMMA blends studied by torque rheometry. *Mater. Sci. Eng. C* **2009**, *29*, 657–661. [CrossRef]
43. Monte, S.J. Neoalkoxy titanate and zirconate coupling agent additives in thermoplastics. *Polym. Polym. Compos.* **2002**, *10*, 121–172. [CrossRef]
44. Agrawal, P.; Rodrigues, A.W.B.; Araújo, E.M.; Mélo, T.J.A. Influence of reactive compatibilizers on the rheometrical and mechanical properties of PA6/LDPE and PA6/HDPE blends. *J. Mater. Sci.* **2010**, *45*, 496–502. [CrossRef]
45. Hong, H.; Li, X.; Liu, H.; Zhang, H.; He, H.; Xu, H.; Jia, D. Transform rice husk and recycled polyethylene into high performance composites: Using a novel compatibilizer to infiltratively enhance the interfacial interactions. *Prog. Rubber Plast. Recycl. Technol.* **2016**, *32*, 253–268. [CrossRef]
46. Awang, M.; Wan Mohd, W.R. Comparative studies of titanium dioxide and zinc oxide as a potential filler in polypropylene reinforced rice husk composite. *IOP Conf. Ser. Mater. Sci. Eng.* **2018**, *342*, 012046. [CrossRef]
47. Chen, R.S.; Ahmad, S. Extrusion processing of a high fibre loading of agrowaste in recycled polyolefin biocomposite. *J. Thermoplast. Compos. Mater.* **2021**, *34*, 40–54. [CrossRef]
48. Chen, R.S.; Ahmad, S.; Gan, S.; Salleh, M.N.; Ab Ghani, M.H.; Tarawneh, M.A. Effect of polymer blend matrix compatibility and fibre reinforcement content on thermal stability and flammability of ecocomposites made from waste materials. *Thermochim. Acta* **2016**, *640*, 52–61. [CrossRef]
49. Chen, R.S.; Ahmad, S. Characterization of Rice Husk Biofibre-Reinforced Recycled Thermoplastic Blend Biocomposite. In *Composites from Renewable and Sustainable Materials*; IntechOpen: London, UK, 2016.
50. Camacho, W.; Karlsson, S. NIR, DSC, and FTIR as quantitative methods for compositional analysis of blends of polymers obtained from recycled mixed plastic waste. *Polym. Eng. Sci.* **2001**, *41*, 1626–1635. [CrossRef]
51. Yao, F.; Wu, Q.; Lei, Y.; Xu, Y. Rice straw fiber-reinforced high-density polyethylene composite: Effect of fiber type and loading. *Ind. Crops Prod.* **2008**, *28*, 63–72. [CrossRef]
52. Abdelwahab, M.A.; Misra, M.; Mohanty, A.K. Injection molded biocomposites from polypropylene and lignin: Effect of compatibilizers on interfacial adhesion and performance. *Ind. Crops Prod.* **2019**, *132*, 497–510. [CrossRef]
53. Pokharel, P.; Bae, H.; Lim, J.G.; Lee, K.Y.; Choi, S. Effects of titanate treatment on morphology and mechanical properties of graphene nanoplatelets/high density polyethylene nanocomposites. *J. Appl. Polym. Sci.* **2015**, *132*, 42073. [CrossRef]
54. Raghu, N.; Kale, A.; Chauhan, S.; Aggarwal, P.K. Rice husk reinforced polypropylene composites: Mechanical, morphological and thermal properties. *J. Indian Acad. Wood Sci.* **2018**, *15*, 96–104. [CrossRef]
55. Chen, R.S.; Ab Ghani, M.H.; Salleh, M.N.; Ahmad, S.; Tarawneh, M.A. Mechanical, water absorption, and morphology of recycled polymer blend rice husk flour biocomposites. *J. Appl. Polym. Sci.* **2015**, *132*, 41494. [CrossRef]
56. Yang, H.S.; Kim, H.J.; Park, H.J.; Lee, B.J.; Hwang, T.S. Effect of compatibilizing agents on rice-husk flour reinforced polypropylene composites. *Compos. Struct.* **2007**, *77*, 45–55. [CrossRef]
57. Sadik, W.A.A.; El Demerdash, A.G.M.; Abbas, R.; Bedir, A. Effect of nanosilica and nanoclay on the mechanical, physical, and morphological properties of recycled linear low density polyethylene/rice husk composites. *J. Polym. Environ.* **2021**, *29*, 1600–1615. [CrossRef]
58. Yang, H.S.; Wolcott, M.P.; Kim, H.S.; Kim, S.; Kim, H.J. Effect of different compatibilizing agents on the mechanical properties of lignocellulosic material filled polyethylene bio-composites. *Compos. Struct.* **2007**, *79*, 369–375. [CrossRef]
59. Rodríguez, C.A.; Medina, J.A.; Reinecke, H. New thermoplastic materials reinforced with cellulose based fibers. *J. Appl. Polym. Sci.* **2003**, *90*, 3466–3472. [CrossRef]